Magnetic ordering in double-chain $PrBa_2Cu_4O_8$

W.-H. Li, S. Y. Wu, Y.-C. Lin, and K. C. Lee
Department of Physics, National Central University, Chung-Li, Taiwan 32054, Republic of China

J. W. Lynn
NIST Center for Neutron Research, NIST, Gaithersburg, Maryland 20899

S. S. Weng, I. P. Hong, J.-Y. Lin,* and H. D. Yang
Department of Physics, National Sun Yat-Sen University, Kaohsiung, Taiwan 80424, Republic of China
(Received 10 September 1998; revised manuscript received 8 March 1999)

We have successfully synthesized a single-phase sample of double-chain $PrBa_2Cu_4O_8$ at ambient oxygen pressure by employing the nitric pyrolysis method. Electrical resistivity, ac magnetic susceptibility, and neutron-diffraction measurements were performed to study the basic magnetic properties of the system. The system displayed metallic conduction, and no superconductivity was observed for temperatures down to 4.2 K. An anomaly was evident in the temperature dependence of the ac susceptibility around 200 K, where a shoulder in the resistivity was also clearly seen. The Pr spins were found to order at 17 K, with a magnetic structure that may be characterized by $\{\frac{1}{2}\frac{1}{2}l\}$ wave vectors with l = whole integers and half integers, showing that the couplings between the Pr spins are antiferromagnetic in nature. Another transition of unknown origin is also evident around 2 K. [S0163-1829(99)03729-7]

I. INTRODUCTION

Among the rare-earth cuprates, the compound $PrBa_2Cu_3O_7$ (Pr123) has distinguished itself from others by its unique properties, such as the absence of superconductivity, the semiconducting electrical behavior, an anomalously high Néel temperature and small saturated moment for the Pr spins, and a relatively large electronic contribution to the specific heat.[1–3] Although the general properties of the related compounds have been intensively investigated, the origins of the distinct properties of single-chain Pr123 and the roles that the chains play remain puzzling. Recently, high quality samples of double-chain $PrBa_2Cu_4O_8$ (Pr124) have been successfully synthesized.[4–7] This provides the opportunity to study the effect of the presence of an extra chain layer on the basic properties of the system. It has been found[8] that the Cu-O bonding in the chain layers in double-chain compounds is much stronger than in single-chain compounds, which results in a much more stable oxygen content against thermal agitation for the former than for the latter. Thermogravimetric analysis has shown that the oxygen content in the Pr124 system remains stable up to 800 °C, whereas it begins to become unstable at 300 °C in the Pr123 systems. The critical content x_c of the Pr ions, where superconductivity is completely suppressed, is much higher in double-chain $Y_{1-x}Pr_xBa_2Cu_4O_8$ ($x_c=0.8$) than that in the single-chain $Y_{1-x}Pr_xBa_2Cu_3O_7$ ($x_c=0.55$).[9,10] In addition, unlike the semiconducting behavior observed in the Pr123 system, Pr124 has been found to be metallic.[10,11] Similar to what has been widely observed in the Pr123 systems,[12] the transition at 17 K, which is generally believed to signify the Pr spin ordering,[2,13] is also present in specific-heat and magnetization measurements made on Pr124 compounds.[10,11]

In this article, we report on the results of studies made on the basic magnetic properties of a polycrystalline $PrBa_2Cu_4O_8$, using resistivity, ac magnetic susceptibility, and neutron-diffraction measurements. Three anomalies at 2, 17 and 200 K are clearly evident in the temperature dependence of the ac susceptibility. The anomaly at 17 K is associated with the ordering of the Pr spins, while that at 200 K may originate from the ordering of the Cu spins. The transition around 2 K is sensitive to an applied dc field, but its origin is not clear at the present time.

II. SAMPLE CHARACTERIZATION

About 7 g of a powder sample of nominal composition $PrBa_2Cu_4O_8$ was prepared at ambient oxygen pressure by employing the nitric pyrolysis method. The details of the sample fabrication procedure can be found in Ref. 7. X-ray-diffraction measurements were used first to characterize the sample. No obvious difference was found among the diffraction patterns taken on the different portions of the sample. The precise crystal structure was then determined by a complete structural analysis using high-resolution neutron-diffraction measurements performed on BT-1, the 32-detector powder diffractometer at the NIST Research Reactor. The high-resolution diffraction patterns covered a range of scattering angles from 3° to 168°, and were collected with the sample loaded in a cylindrical aluminum can. A Cu(311) monochromator crystal was used to select a wavelength of $\lambda=1.5401$ Å for the incident neutrons. Angular collimators with horizontal divergences of 15′, 20′, and 7′ full width at half maximum (FWHM) acceptance were employed for the in-pile, monochromatic, and diffracted beams, respectively.

The diffraction pattern was analyzed using the general structure analysis system (GSAS) program of Larson and Von Dreele,[14] in which the Rietveld refinement method[15,16] was followed. In the refinement process, the portions of the

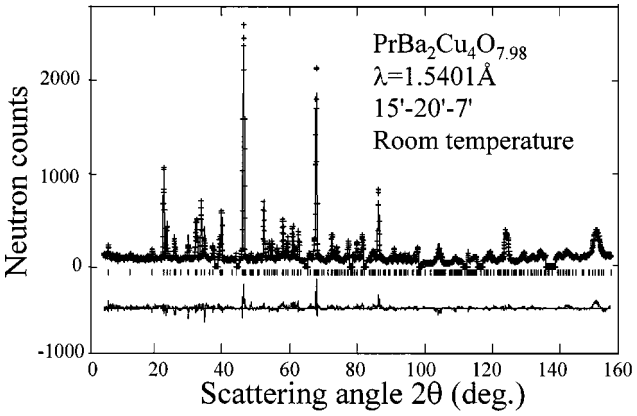

FIG. 1. Observed (crosses) and fitted (solid lines) neutron powder diffraction pattern collected at room temperature, where their differences are plotted at the bottom. The short vertical lines shown below the pattern mark the calculated positions of the Bragg reflections.

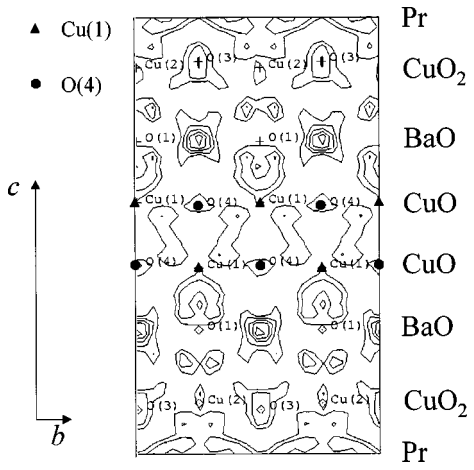

FIG. 2. A portion of the difference density map viewed along the *a*-axis direction. The upper-half and the lower-half planes are identical but shifted, one respect to the other, by $(0\frac{1}{2}0)$. Clearly, each O(4) ion is bound to three Cu(1) ions.

diffraction patterns containing peaks from the aluminum sample holder were excluded. Several models with different symmetries were assumed in the preliminary analysis. The final refinement was carried out assuming the symmetry of space group *Ammm*, with a structure consisting of two (Pr123+CuO) blocks stacked one on top of the other but shifted by $\frac{1}{2}b$ as suggested in previous studies.[17,18] All structural and lattice parameters were allowed to vary simultaneously, and R_W, the weighted R factor,[16] differed by less than one part in a thousand in two successive cycles.

Figure 1 shows the observed and fitted patterns taken at room temperature, with their differences plotted at the bottom. Clearly, the calculated and the observed patterns agree very well, showing that the proposed structure is correct. Careful analysis of the occupancy factors of the oxygen atoms shows that the oxygen sites are almost full with an oxygen content of 7.98(2) for the compound, which gives a chemical formula of $PrBa_2Cu_4O_{7.98}$ for the compound. The compound crystallized into an orthorhombic structure of lattice constants $a=3.8875(2)$ Å, $b=3.9041(2)$ Å, and $c=27.3423(16)$ Å at room temperature. Table I lists the refined structural parameters, where the center of the unit cell is defined to be at a Pr site. Figure 2 shows a portion of the difference density map viewed along the *a*-axis direction, where the triangles and the circles mark, respectively, the Cu(1) and O(4) atoms in the CuO-chain layers. The map shown covers a size of 7.81×13.67 Å, and the contours are drawn at densities of 17, 13, 9, 5, and 1 Å^3 from inside out. Clearly, the upper-half and the lower-half planes are identical but shifted, one respect to the other, by $(0\frac{1}{2}0)$, such that each O(4) is bounded to three Cu(1) ions which results in a much more stable oxygen content for the 124 compounds than for the 123 compounds. In addition, this analysis was also directed at searching for impurity phases, especially for the Pr123 phase. No trace of impurity phases such as $PrBa_2Cu_3O_7$, $PrBaO_3$, $PrCuO_3$, $BaCuO_3$, and CuO_2 were found, showing that this sample is essentially single phase. We estimated that any impurity phases in the sample are less than 2%.

III. EXPERIMENTAL DETAILS

Electrical resistivity, ac magnetic susceptibility, and neutron-diffraction measurements were all performed to

TABLE I. Refined structural parameters of $PrBa_2Cu_4O_{7.98}$ at room temperature, where B represents the isotropic temperature parameter.

$PrBa_2Cu_4O_{7.98}$, space group *Ammm*, room temperature $a=3.887\,51(20)$ Å, $b=3.904\,14(23)$ Å, $c=27.3423(16)$ Å					
Atom	x	y	z	B (Å^2)	Occupancy
Pr	0.5	0.5	0	1.98(9)	1
Cu(2)	0	0	0.0640(1)	2.49(9)	1
O(2)	0.5	0	0.0565(3)	2.69(6)	1
O(3)	0	0.5	0.0570(3)	3.77(8)	1
Ba	0.5	0.5	0.1382(2)	1.72(5)	1
O(1)	0	0	0.1450(1)	2.73(6)	1
Cu(1)	0	0	0.2135(1)	2.47(8)	1
O(4)	0	0.5	0.2168(2)	2.50(8)	0.99(1)
$R_p(\%)=9.66$		$R_W(\%)=12.38$		$\chi=1.823$	

study the basic magnetic properties of the system. Resistivity was measured employing the standard four-probe method in the temperature range of 78–260 K with leads evaporated on a sintered pellet. The ac susceptibility measurements were performed using a conventional ac susceptometer. In these measurements, the sample was subjected to a weak driving ac magnetic field, with and without an applied dc field, and the response of the system was then measured using two identical sensing coils connected in opposition. During these measurements, ~1 g of the sample was loaded in a cylindrical plastic container, and both the in-phase and out-of-phase components were measured. A pumped ^{4}He cryostat was used to cool the sample, and the lowest temperature obtained was 2.1 K.

The neutron magnetic diffraction experiments were conducted at the NIST Research Reactor, using the BT-9 triple-axis spectrometer operated in the double-axis mode without using an analyzer crystal. A neutron wavelength of $\lambda = 2.351$ Å, defined using a pyrolytic graphite PG (002) monochromator crystal, was employed. Collimators with horizontal divergences of 40′, 48′, and 48′ FWHM acceptance were used for the in-pile, monochromatic, and diffracted beams, respectively. For these measurements, ~7 g of the sample was loaded in a cylindrical aluminum can filled with helium exchange gas to facilitate thermal conduction. The sample was cooled using a pumped ^{4}He cryostat operated between 1.6 and 250 K.

IV. RESULTS AND DISCUSSION

The temperature dependence of the ac susceptibility, measured using driving fields of various strengths and frequencies, was determined first to study the basic magnetic response of the system. In employing such a technique one has the advantage that the measurements can be performed with an extremely weak probing field, which then reveals the intrinsic properties of the system excluding effects that might be induced by the applied field. Neutron-diffraction patterns covering certain temperature regimes, where the susceptibility shows anomalies, were then collected to search for magnetic signals.

A. Pr spin ordering

Shown in Fig. 3 is the temperature dependence of the in-phase component of the ac susceptibility $\chi(T)$ measured using a weak driving field of rms strength 1 Oe and frequency 1000 Hz. This $\chi(T)$ observed for the double-chain Pr124 is very similar to that for the single-chain Pr123. The main feature seen is the inflection point at 17 K, which we believe is associated with the ordering of the Pr spins (see below). This anomaly occurs at almost the same temperature at which the Pr spins in Pr123 order,[2] irrespective of the difference in their chain structure. Below 17 K, $\chi(T)$ increases as the temperature is further reduced to the lowest temperature studied of $T = 2.1$ K. This behavior is similar to what is usually observed in other Pr containing high-T_c systems, where the cusp in $\chi(T)$ anticipated for antiferromagnetic ordering of the Pr spins is not seen.

In Fig. 4 we show the magnetic diffraction pattern obtained at 6 K, where the diffraction pattern taken at 22 K,

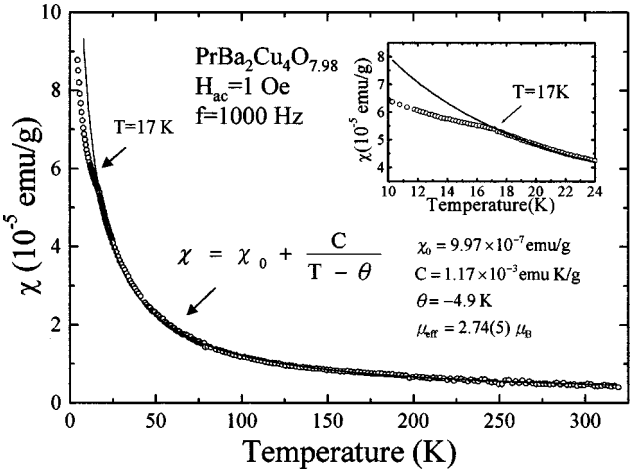

FIG. 3. Temperature dependence of the in-phase component of the ac susceptibility measured using a weak driving field of rms strength 1 Oe and frequency 1000 Hz. A transition is clearly evident at 17 K, which is associated with the Pr spin ordering. The solid line shown is a fit of the data obtained between $25 < T < 180$ K to the Curie-Weiss expression.

which serves as the nonmagnetic background, has been subtracted from the data to isolate the magnetic signal. Three magnetic peaks at the $\{\frac{1}{2}\frac{1}{2}\frac{1}{2}\}$, $\{\frac{1}{2}\frac{1}{2}\frac{3}{2}\}$, and $\{\frac{1}{2}\frac{1}{2}2\}$ positions, as indexed based on the nuclear unit cell, are seen. We denote the $\{\frac{1}{2}\frac{1}{2}l\}$-type of reflections with l = half integer and l = whole integer as the half-integral and whole-integral peaks, respectively. Clearly, both half-integral peaks and whole-integral peaks are observed. The appearance of the $\{\frac{1}{2}\frac{1}{2}2\}$ peak strongly suggests the existence of other whole-integral peaks, such as $\{\frac{1}{2}\frac{1}{2}0\}$ and $\{\frac{1}{2}\frac{1}{2}1\}$ reflections. Unfortunately, the expected angular separations among the $\{\frac{1}{2}\frac{1}{2}0\}$, $\{\frac{1}{2}\frac{1}{2}\frac{1}{2}\}$, and $\{\frac{1}{2}\frac{1}{2}1\}$ reflections are less than 0.3°. This makes it difficult to separate them with the present instrumental resolution, while the weak intensities make it impractical to improve the angular resolution significantly. It is thus possible that each peak observed might contain more than one reflection.

The Pr ions form a base-centered (b-c plane in our notation) orthorhombic sublattice, hence a triangular lattice in the

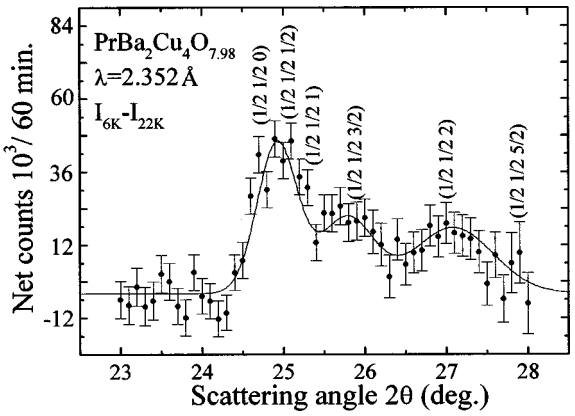

FIG. 4. Magnetic diffraction pattern obtained at 6 K, where the indices shown are based on the nuclear unit cell. The solid curves shown are the fit of the data to the proposed structure, using a Gaussian resolution function for the peak profiles.

b-c plane, where the nearest-neighbor distance between the Pr ions in the c-axis direction is a factor of about 3.5 longer than that in the a-b plane. Thus in the 124 materials the magnetic interactions along the c axis are much weaker than within the a-b plane, leading to two-dimensional behavior for the rare-earth magnetic system.[19] There are two Pr ions in the magnetic unit cell along both the a and b axes, and the simplest arrangement for the Pr spins in the a-b planes is that the nearest-neighbor Pr spins are aligned antiparallel, as has been observed for many of the rare earths in the layered cuprates. The presence of the half-integral peaks indicates that the magnetic unit cell is double the nuclear one along all three crystallographic directions and all the couplings between the Pr spins are thus antiferromagnetic in nature. A collinear structure then gives a zero net interaction between layers (a-b plane), making the net c-axis interaction extremely weak. In the Dy124 material, for example, this renders the magnetism truly two dimensional.[20] In the present case we have both half-integral and whole-integral peaks, rather than just a two-dimensional profile, which clearly indicates that there is ordering along the c axis. These two types of peaks could belong to separate magnetic structures (macroscopically), as the delicate balance of interactions has been found to very sensitive to the metallurgical state of the sample.[21] Alternatively, the two types of peaks could originate from the same region of the sample, indicating a noncollinear structure for the Pr spins. If this is the case, the presence of both types of peaks would indicate that the two base-centered Pr spins cannot simply point in opposite directions. Based on these constraints, model calculations were performed using the intensity formula[22,23] for noncollinear spin structures. Two spin configurations, one collinear and the other noncollinear, were found to fit reasonably well to the observed patterns, with the goodness of the fit of the noncollinear one about 8% better than that of the collinear one. Their configurations in the b-c plane are shown in Fig. 5(a) (collinear) and Fig. 5(b) (noncollinear), where the scale used for the b axis is expanded by a factor of two for clarity of presentation. For the noncollinear structure, the spin arrangements in the two adjacent layers are quite different: in one layer it is collinear, whereas in the other it is strongly canted and noncollinear. This is improbable since the Pr sites are in identical local environments, and a similar spin structure in each layer may be anticipated. Allowing the Pr spins in the $z=0$ and $z=1$ planes to depart from being exactly antiparallel resulted in poorer fits (even poorer than the collinear configuration). We therefore favor the collinear structure shown in Fig. 6, even though the fit is not quite as good as the noncollinear one.

In the present calculation any coupling of the Pr to the Cu magnetic structure was not considered. Pr-Cu coupling has been observed[13,24–27] in the 123 systems, and can cause a counter rotation of the Cu spin axes as the Pr spins order. However, the details of the magnetic structures and this coupling are quite different in doped[24,26,28] and high-purity crystals[27] and powders.[2,13] In the present case any ordered Cu moment is small, the magnetic structure is not known, it is not known if the chain-type Cu ions carry a moment, and there is no firm evidence yet to support any Pr-Cu coupling for the 124 systems. We therefore have not included a contribution from the Cu spins in the calculation. We remark

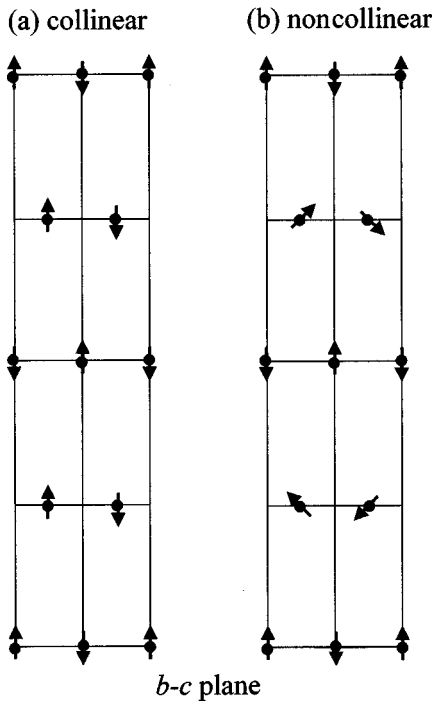

FIG. 5. Configurations of the Pr spins in the b-c plane for the two magnetic structures found that fit reasonably well to the data.

that the observed Curie-Weiss behavior for the high-temperature $\chi(T)$ (see below) alone is not strong enough evidence, we believe, to conclude a Pr-Cu coupling in the present Pr124 system. The solid curve shown in Fig. 4 is the calculated intensity based on the proposed structure, with a saturated moment $\langle \mu_Z \rangle = 0.66(4)\mu_B$ (obtained by comparing

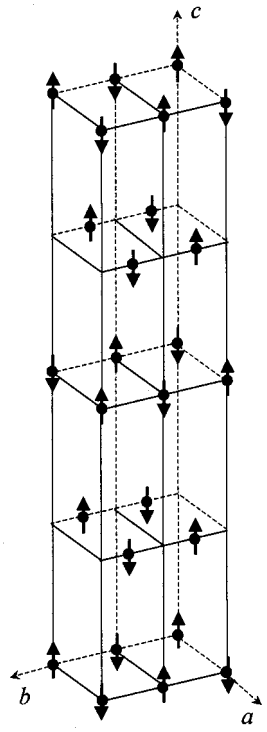

FIG. 6. The proposed magnetic structure for the Pr spins in $PrBa_2Cu_4O_8$, where the nearest-neighbor Pr spins in the basal a-b plane are aligned antiparallel.

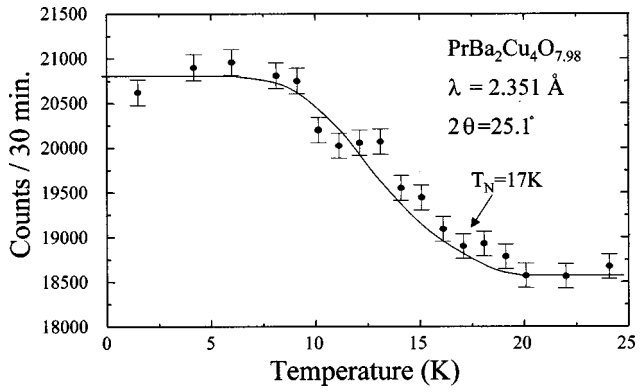

FIG. 7. Temperature dependence of the peak intensity at the $\{\frac{1}{2}\frac{1}{2}\frac{1}{2}\}$ position, showing the variation of the square of the staggered magnetization with temperature. The Néel temperature of the Pr spins is $T_N \approx 17$ K.

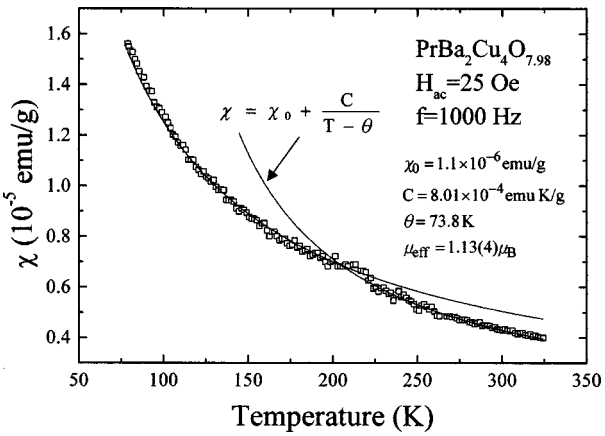

FIG. 8. Temperature dependence of the in-phase component of the ac susceptibility measured with a driving field of rms strength 25 Oe and frequency 1000 Hz. An inflection point is clearly evident at 200 K, showing that a phase transition occurs at this temperature.

the magnetic intensities to the nuclear ones). This saturated moment found for the Pr spins in Pr124 is about 10% smaller than what was found[2] for the Pr spins in Pr123. We remark that this proposed structure for the Pr spins is not quite the same as the one proposed in a separate study,[29] where only whole-integral peaks were observed that suggested the Pr spins along the *c*-axis direction are parallel. This may be related to small differences in the oxygen concentration, as has been widely observed in other high-T_C compounds.[21]

In Fig. 7 we show the temperature dependence of the peak intensity at the $\{\frac{1}{2}\frac{1}{2}\frac{1}{2}\}$ position, where the solid curve is only a guide for the eye. This plot shows the variation of the square of the magnetization with temperature, and reveals a typical order-parameter curve for a polycrystalline sample. The ordering temperature of the Pr spins, as determined by the inflection point of the order-parameter curve, is $T_N \approx 17$ K, which matches the temperature at which $\chi(T)$ shows an anomaly. This ordering temperature found for the Pr spins in Pr124 is essentially the same temperature at which the Pr spins order in Pr123 despite the difference in their spin structures. It is expected that the ordering temperature would be similar, since the coupling within the a-b plane should dominate the Pr spin ordering, and the ordering temperature is mainly determined by the coupling strength in these planes as expected from the anisotropic crystal structure of these materials.

B. High-temperature transition

Above T_N, $\chi(T)$ may be described using the Curie-Weiss law for antiferromagnetic coupling, which is mainly contributed by the paramagnetic Pr spins. The solid curve shown in Fig. 3 is the fit of the data between 25 and 180 K to the expression $\chi_0 + C/(T-\theta)$, where C and θ are the Curie-Weiss constant and Curie-Weiss temperature, respectively, and the temperature independent term χ_0 represents the paramagnetic contribution from the conduction electrons. The fitted values are listed in Fig. 3. A negative value of $\theta = -4.9$ K was obtained from the fit, indicating an antiferromagnetic character for the Pr spins which agrees with the neutron-diffraction results. Calculation of the effective moment using the fitted value for C gives $\mu_{\text{eff}} = 2.74(5)\mu_B$, which is only 8% larger than the value of $2.54\mu_B$ expected for the free Pr^{4+} ions and is much below the value of $3.58\mu_B$ for the free Pr^{3+}. Note that similar values are usually obtained for the Pr in Pr123 systems[3] as well, suggesting that the paramagnetic behavior of Pr in Pr123 and in Pr124 systems is alike. We believe that the splitting of the free-ion ground-state term by the crystal field and hybridization between the Pr $4f$ and O $2p$ orbitals plays an essential role in the reduction of the effective moment.

If the fit is performed using the data obtained between 25 and 320 K, a difference of ~4% in all fitted values results. The reason that we choose to use the data between 25 and 180 K to find the Curie-Weiss parameters for the paramagnetic Pr can be seen in Fig. 8, where $\chi(T)$ measured using a stronger driving field with an rms strength of 25 Oe is shown. An anomaly is clearly evident at 200 K, signaling that a phase transition occurs at this temperature. $\chi(T)$ for temperatures above and below 200 K follow separate Curie-Weiss curves. The separation becomes larger if a stronger driving field is used. In Fig. 8, the solid curve in the low-temperature data is the same curve shown in Fig. 3, and the solid curve in the high-temperature data is a fit of the data obtained between 230 and 320 K to the Curie-Weiss expression.

The transition at 200 K is also evident in the temperature dependence of the resistivity $\rho(T)$ shown in Fig. 9. This resistivity observed for the Pr124 is about two orders-of-magnitude smaller than what is usually observed for the Pr123 systems. The basic transport property of Pr124 is metallic but a shoulder appears around 200 K, which agrees with what is observed in other studies.[4,11] This observation is in sharp contrast with what is observed[30,31] for the Pr123 system, where semiconducting behavior is seen. It has been well established that both the single CuO chain in Y123 and the double CuO chains in Y124 are metallic.[32–34] NMR and nuclear quadrupole resonance (NQR) measurements have shown that the spin susceptibilities of the CuO_2 planes and CuO chains are markedly different, suggesting that these two conducting channels may act independently.[35,36] Both the Pr123 and Pr124 contain the same CuO_2-Pr-CuO_2 layers. The major differences are due to their chain structure. It is then the chain structure that is mainly responsible for the

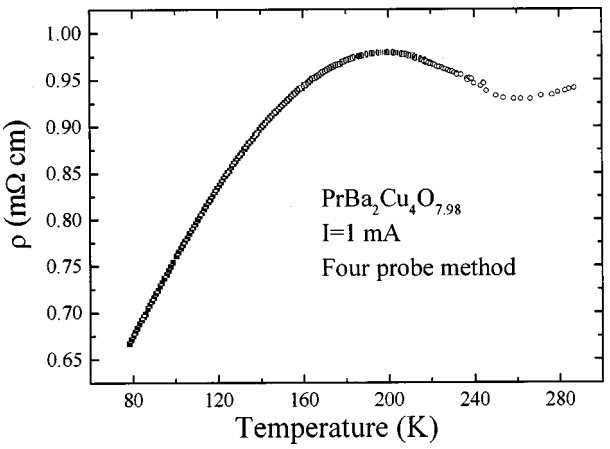

FIG. 9. Variation of the resistivity with temperature, showing that the basic transport property of the Pr124 is metallic, however, a shoulder is evident around 200 K.

difference in the transport behavior between Pr123 and Pr124. Apparently, double chains are capable of supporting significant conductivity, which in turn gives rise to a metallic conduction.

No structural change was observed between 1.6 and 300 K. One possible origin for the transition at around 200 K is that it is associated with the ordering of the moments on Cu, as has been suggested[37] in NMR and muon-spin-relaxation measurements and has been observed[27] in Pr123 single crystals. We note that the expected magnetic intensities associated with the Cu ordering are smaller than those associated with the Pr spins, since a smaller moment for the Cu is anticipated. The difference between the neutron-diffraction patterns taken at 150 and 240 K does show small magnetic signals at the positions of the half-integral peaks. Unfortunately, based on our powder neutron data no definitive conclusion can be made at the present time, due to the large error bars for the observed signals, and it may not be feasible to study this issue using powder samples. Measurements using single crystals are likely necessary before definitive conclusions can be drawn concerning the origin of this transition. We further note that a Curie-Weiss $\chi(T)$ is also expected for a noninteracting two-component paramagnetic system.[38,39] If the Cu spins do order at 200 K, the observed Curie-Weiss $\chi(T)$ above 200 K is then contributed by both the paramagnetic Pr and paramagnetic Cu moments. Treating these two components as being statistically independent[38] and using the paramagnetic parameter obtained at low temperatures for the Pr moment, we then obtained an effective moment of $\mu_{\text{eff}}=0.99(4)\mu_B$ for the Cu. This value seems reasonable for Cu moments, and is close to the value of $1.24\mu_B$ expected for the free Cu^{2+} ions.

C. Low temperature transition

At low temperatures, another transition is evident. In Fig. 10 we show the low-temperature portions of the $\chi(T)$ and $d\chi/dT$ measured with applied dc magnetic fields. Above 17 K, $\chi(T)$ is essentially not affected by the applied field, showing that 10 kOe is not strong enough to alter the paramagnetic Pr spins. Below 17 K, χ is suppressed by an applied field, and the $\chi(T)$ measured with different applied fields

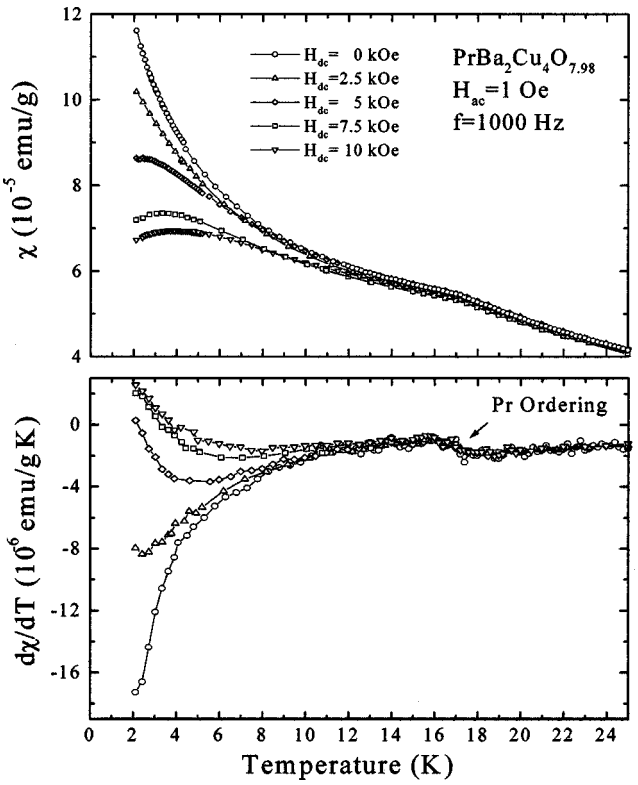

FIG. 10. Effects of an applied dc field on $\chi(T)$. Above 17 K, $\chi(T)$ is essentially unaffected by the applied field, while $\chi(T)$ is suppressed below 17 K. Cusps in $\chi(T)$ are clearly evident in the $H_{\text{dc}}\geqslant 5$ kOe curves.

depart from each other. Cusps in $\chi(T)$ are clearly evident in the $H_{\text{dc}}\geqslant 5$ kOe curves. We may expect that a cusp should also be presented in the $\chi(T)$ measured with a smaller applied field if the temperature is further reduced, as the $d\chi/dT$ for the $H_{\text{dc}}=0$ curve begins to show an upturn at 2.1 K, the lowest temperature achieved in this study. Specific-heat[11] and resistivity[5] measurements performed in other studies also reveal anomalies at these temperatures. Naturally, one could ask whether this is associated with the Pr spin ordering or a separate transition. First, a ferromagnetic character for the transition at low temperature is suggested as the peak position shifts to higher temperature when the strength of the applied field is increased, while the coupling between the Pr spins is antiferromagnetic in nature as shown above. Second, $d\chi/dT$ shown in Fig. 10 indicates that the low-temperature transition occurs below 5 K, while the order parameter data shown in Fig. 7 reveals that the Pr ordering saturates around 8 K. These observed phenomena lead us to believe that this low-temperature anomaly is associated with a transition other than the Pr spin ordering at $T_N\approx 17$ K. It is also unlikely to be associated with the type of change in the spin structure observed in high-purity single crystals,[27] since in that case at low temperature the structure along the c axis becomes fully antiferromagnetic. This transition is also observed in zero-field measurements of both the resistivity[5] and specific-heat[11] measurements. Without an applied field the peak in $\chi(T)$ is expected to appear at 1.5 K by extrapolation. No magnetic signal was observed to develop between the neutron-diffraction patterns taken at 1.6 K (lowest temperature available in this study) and 6 K. We remark that an

anomaly at 5 K in both the specific-heat and susceptibility data was also seen[2] in the Pr123 system. Its origin remains to be clarified.

V. CONCLUSION

In summary, double-chain $PrBa_2Cu_4O_{7.98}$ has been successfully synthesized using the nitric pyrolysis method at ambient oxygen pressure. The compound crystallizes into an orthorhombic symmetry of space group *Ammm*. No structural phase transition was observed in the temperature range of 1.6–320 K. The system displays metallic conduction, which we believe is mainly attributed to the double-CuO chains. An anomaly is evident at around 200 K in both the ac susceptibility and resistivity, which could be associated with the ordering of the Cu spins. The coupling between the Pr spins is antiferromagnetic in nature, and they order at 17 K with a collinear structure. Apparently, the presence of an extra chain layer and a triangular spatial arrangement for the Pr spins in the *b*-*c* plane does not significantly alter the ordering temperature of Pr. The coupling within the basal plane dominates the Pr magnetism, as expected from the anisotropic crystal structure of this class of materials. Similar to what has been observed in the Pr123 system, there is another transition that occurs at a lower temperature, whose origin remains to be clarified.

ACKNOWLEDGMENTS

Identification of commercial equipment in the text is not intended to imply recommendation of endorsement by the National Institute of Standards and Technology. The work at NCU was supported by the National Science Council of the Republic of China under Grant No. NSC 88-2112-M-008-002. The work at NSYSU was supported by the National Science Council of the Republic of China under Grant No. NSC 88-2112-M-110-007.

*Current address: Institute of Physics, National Chaio-Tung University, Hsin-Chu, Taiwan 710, Republic of China.

[1] A. Kebede, C. S. Jee, J. Schegler, J. W. Crow, T. Mihalisin, G. H. Myer, R. E. Salomom, P. Schlottmann, M. V. Kuric, S. H. Bloom, and R. P. Guertin, Phys. Rev. B **40**, 4453 (1989).

[2] W.-H. Li, J. W. Lynn, S. Skanthakumar, T. W. Clinton, A. Kebede, C.-S. Jee, J. E. Crow, and T. Mihalisin, Phys. Rev. B **40**, 5300 (1989).

[3] H. B. Radousky, J. Mater. Res. **7**, 1917 (1992).

[4] N. Seiji, S. Adachi, and H. Yamauchi, Physica C **227**, 377 (1994).

[5] Y. Yamada, S. Horii, N. Yamada, Z. Guo, Y. Kodama, K. Kawamoto, U. Mizuyani, and I. Hirabayashi, Physica C **231**, 131 (1994).

[6] M. Kall, A. P. Litvinchuk, P. Berastegui, L. G. Johansson, L. Borjesson, M. Kakihana, and Osada, Phys. Rev. B **53**, 3590 (1996).

[7] C. W. Lin, J.-Y. Lin, H. D. Yang, T. H. Meen, H. L. Tsay, Y. C. Chen, J. C. Huang, S. R. Sheen, M. K. Wu, Physica C **276**, 225 (1997).

[8] J. Karpinski, E. Kaldis, E. Jilek, S. Rusiecki, and B. Bucher, Nature (London) **341**, 41 (1989).

[9] D. E. Morris, J. H. Nickel, J. Y. T. Wei, N. G. Asmar, J. S. Scott, U. M. Scheven, C. T. Hultgren, A. G. Markelz, J. E. Post, P. J. Heaney, D. R. Veblen, and R. M. Hazen, Phys. Rev. B **39**, 7347 (1989).

[10] Z. Guo, N. Yamada, K. Ichiro, T. Iri, and K. Kohn, Physica C **220**, 41 (1994).

[11] H. D. Yang, J.-L. Lin, S. S. Weng, C. W. Lin, H. L. Tsay, Y. C. Chen, T. H. Meen, T. I. Hsu, and H. C. Ku, Phys. Rev. B **56**, 14 180 (1997).

[12] For a recent review, see J. W. Lynn, J. Alloys Compd. **250**, 552 (1997).

[13] S. Skanthakumar, J. W. Lynn, N. Rosov, G. Cao, and J. E. Crow, Phys. Rev. B **55**, 3406 (1997).

[14] A. C. Larson and R. B. Von Dreele, Los Alamos National Laboratory, Report No. LA-UR-86-748, 1990 (unpublished).

[15] H. M. Rietveld, J. Appl. Crystallogr. **2**, 65 (1969).

[16] *The Rietveld Method*, edited by R. A. Young (Oxford University Press, New York, 1993).

[17] H. W. Zandbergen, R. Gronsky, K. Wang, and G. Thomas, Nature (London) **331**, 596 (1988).

[18] P. Berasengui, L. G. Johenssum, M. Kall, and L. Bereson, Physica C **201**, 147 (1992).

[19] J. W. Lynn, J. Alloys Compd. **181**, 419 (1992).

[20] H. Zhang, J. W. Lynn, W.-H. Li, T. W. Clinton, and D. E. Morris, Phys. Rev. B **41**, 11 229 (1990).

[21] See, for example, T. W. Clinton, J. W. Lynn, J. Z. Liu, Y. X. Jia, T. J. Goodwin, R. N. Shelton, B. W. Lee, M. Buchgeister, M. B. Maple, and J. L. Peng, Phys. Rev. B **51**, 15 429 (1995).

[22] J. W. Lynn, G. Shirane, and M. B. Blume, Phys. Rev. Lett. **37**, 154 (1976).

[23] G. L. Squires, *Introduction to the Theory of Thermal Neutron Scattering* (Cambridge University Press, Cambridge, 1976).

[24] A. Longmore, A. T. Boothroyd, C. Changkang, H. Yongle, M. P. Nutley, N. H. Andersen, H. Casalta, P. Schleger, and A. N. Christensen, Phys. Rev. B **53**, 9382 (1996); A. T. Boothroyd, A. Longmore, N. H. Andersen, E. Brecht, and T. Wolf, Phys. Rev. Lett. **78**, 130 (1997).

[25] A. T. Boothroyd, Physica B **241-243**, 792 (1998).

[26] J. P. Hill, A. T. Boothroyd, N. H. Andersen, E. Brecht, and Th. Wolf, Phys. Rev. B **58**, 11 211 (1998).

[27] S. Uma, W. Schnelle, E. Gmelin, G. Rangarajan, S. Skanthakuma, J. W. Lynn, R. Walter, T. Lorenz, B. Buchner, E. Walker, and A. Erb, J. Phys.: Condens. Matter **10**, L33 (1998).

[28] N. Rosov, J. W. Lynn, G. Cao, J. W. O'Reilly, P. Pernambuco-Wise, and J. E. Crow, Physica C **204**, 171 (1992).

[29] Y.-C. Lin, S. Y. Wu, W.-H. Li, K. C. Lee, J. W. Lynn, C. W. Lin, J.-Y. Lin, and H. D. Yang, Physica B **241-243**, 702 (1998).

[30] B. Okai, K. Takahashi, H. Nozaki, M. Saeki, M. Kosuge, and M. Ohta, Jpn. J. Appl. Phys., Part 2 **26**, L1648 (1987).

[31] J. L. Peng, P. Klavins, R. N. Shelton, H. B. Radousky, P. A. Hahn, and L. Bernardez, Phys. Rev. B **40**, 4517 (1989).

[32] R. Gagnon, C. Lupien, and L. Taillefer, Phys. Rev. B **50**, 3458 (1994).

[33] B. Bucher and P. Watcher, Phys. Rev. B **51**, 3309 (1995); N. E. Hussey, K. Nozawa, H. Takagi, S. Adachi, and K. Tanabe, *ibid.* **56**, R11 423 (1997).

[34] H. Zimmermann, M. Mali, D. Brinkmann, J. Karpinski, E. Kalidas, and S. Rusiecki, Physica C **159**, 681 (1989).

[35] T. Machi, I. Tomano, T. Miyatake, N. Koshizuka, S. Tanaka, T. Imai, and H. Yasuoka, Physica C **173**, 32 (1991).
[36] M. Bankay, M. Mali, J. Roos, and D. Brinkmann, Phys. Rev. B **50**, 6416 (1994).
[37] I. Terasaki, N. Seiji, S. Adachi, and H. Yamauchi, Phys. Rev. B **54**, 11 993 (1996), and references therein.
[38] J. S. Smart, *Effective Field Theories of Magnetism* (W. B. Saunders Press, London, 1966).
[39] M. Tovar, J. Appl. Phys. **83**, 7201 (1998).